Short communication

Bubble coalescence in non-Newtonian fluids in a microfluidic expansion device

CrossMark

Taotao Fu[a,b], Youguang Ma[a,*], Huai Z. Li[b]

[a] State Key Laboratory of Chemical Engineering, Collaborative Innovation Center of Chemical Science and Engineering (Tianjin), School of Chemical Engineering and Technology, Tianjin University, Tianjin 300072, China
[b] Laboratory of Reactions and Process Engineering, University of Lorraine, CNRS, 1, rue Grandville, BP 20451, 54001 Nancy cedex, France

A R T I C L E   I N F O

A B S T R A C T

This communication presents experimentally the bubble coalescence in a microfluidic expansion device using a high-speed digital camera and a micro-particle image velocimetry (micro-PIV) system. Experiments were conducted in a PMMA microchannel of 400 μm deep, composed of an expansion with an angle of 60°. N_2 bubbles were generated in 0.5 wt% polyacrylamide (PAAm) non-Newtonian fluids by hydrodynamic flow-focusing method and flowed past the expansion section. Two different mechanisms for bubble coalescence were observed by changing the gas and liquid flow rates. Three various processes of bubble coalescence were presented and analyzed. The probability, time and position for bubble coalescence were also calculated. The velocity fields in the liquid phase around the aligned bubbles were determined by micro-PIV measurements to gain insight into the mechanism for bubble coalescence.

© 2015 Elsevier B.V. All rights reserved.

1. Introduction

Bubble/droplet interactions are important in a large number of industrial applications, such as emulsion stability, ink-jet printing, coating applications, polymer processing technology, foaming dynamics, fermentation and dynamics of multiphase flows. Among these intrinsic dynamic behaviors, bubble/droplet coalescence is thought to be a key factor for mass/heat transfer and chemical reactions [1,2]. Many investigations have been devoted to bubble/droplet coalescence in conventional columns in both Newtonian and non-Newtonian fluids. Liquid phase properties, gas distribution manners and surfactants play important roles on hydrodynamics of bubble/droplet coalescence. The bubble coalescence process is usually divided into three stages: the acceleration and elongation of the trailing bubble; the trailing bubble catching up with the leading bubble; drainage, thinning, and rupture of the thin film between the two bubbles [3]. For droplet coalescence with a variable viscosity and a colloid-polymer mixture displaying an ultra low surface tension, the coalescence dynamics of droplets is driven by surface tension and slowed down by the viscosity for low Reynolds numbers and by inertia for high Reynolds numbers [4]. For the coalescence of thin liquid dodecane lenses, a conversion of interfacial energy into kinetic energy of flow is

involved [5]. Some methods were employed to study the coalescence of bubbles/droplets, such as electrical fields and external flow [6].

Nowadays, microfluidic devices emerge in many scientific and industrial applications. Multiphase flows are always encountered for enhancing and extending the performance of microfluidic systems [7]. Experimental studies have been focused on the effects of confinement on bubble/droplet breakup and deformation [8–10]. The ability to controllably merge bubble/droplet within segmented flow systems is of high importance in chemical and biological applications [11,12]. In order to realize successful droplet-based devices, multiple "unit operation" must be integrated, including generation of droplets, fission, sorting and mixing within droplets [13,14]. Chen et al. [7] investigated experimentally the effect of confinement on the coalescence of Newtonian droplets in a Newtonian matrix in shear flow and showed that confinement clearly promotes coalescence. Some researchers have provided several efficient methods for bubble/droplet coalescence in microfluidics without external forces. To avoid special channel treatment, electrical field or laser were employed to induce droplet fusion for biological or chemical applications [15]. Niu et al. [11] provided a novel method to merge droplets within segmented flow in microfluidic devices by installing rows of separated pillars in a microfluidic network, and showed that the coalescence is controllable and is dependent of the droplet size. Tan et al. [16] described a geometrically mediated flow to fuse identical droplets in large quantities through rearranging the droplets in microchannels.

* Corresponding author. Fax.: +86 22 27404772.
  E-mail address: ygma@tju.edu.cn (Y. Ma).

Several methods have been employed to evaluate the influence of the distribution of surfactants covered on the interface of droplets on the coalescence of droplets in microfluidic devices. Mazutis and Griffiths [17] presented a microfluidic approach to control selectively droplet coalescence in an expansion section, and showed that the droplet coalescence efficiency is dependent of the contact time between droplets and the interfacial surfactant coverage of droplets. Tullis et al. [18] demonstrated a robust method to make coalescence of anchored droplets by removal of surfactant from the interface of droplet by reducing the concentration of surfactant in the flowing external oil phase. Deng et al. [19] reported an efficient strategy for inducing coalescence of surfactant-covered droplets in converging microchannels by using a micro-lancet with suitable surface wettability to cause temporarily local scattering of surfactants. Krebs et al. [20] studied droplet stability in a microfluidic expansion channel to monitor emulsion stability upon shear-induced collisions, and found that emulsions are stable against coalescence for surfactant SDS concentration less than 10^{-6} M in the residence time of droplets in microchannels without adding NaCl. They also found that the adding of NaCl into the bulk flow can make the emulsions displayed a transition from stable regime to unstable regime, when the NaCl bulk concentration changed from 0.1 M to 0.3 M.

To describe clearly the coalescence event of a droplet pair, Bremond et al. [21] performed experiments to investigate the life of a large number of droplet pairs and focused on the destabilization process of an emulsion in a simply expanding microchannel, and they found that coalescence occurs during the separation stage rather than during the impact stage. Krebs et al. [22] employed a microfluidic circuits to observe on-line the coalescence of oil droplets dispersed in water, and obtained the coalescence time, as well as its relevance to the droplet velocity and diameter. They also found that the coalescence time decreases with the increase of the capillary number and increases with the increase of the viscosity of the dispersed phase [23]. Jose and Cubaud [24] performed experiments on droplet trains in a diverging/converging microfluidic channel, and found that the onset of droplet coalescence was depended on the capillary number based on the viscosity of the continuous phase and the flow rates of both phases. It is evidenced from the above analyses that the coalescence of droplet is relevant to the viscosity of the fluids and fluid hydrodynamics. This is also true for bubble coalescence in microfluidic devices for only several studies at hands. Yang et al. [25] studied experimentally the bubble coalescence in a T-junction microfluidic device and found that the bubble coalescence can be prevented by increasing the liquid viscosity. Wu et al. [26] observed experimentally colliding coalescence and squeezing coalescence of bubble pairs at a T-junction, and demonstrated that the coalescence efficiency was relevant to the liquid velocity and viscosity. It should be pointed out that the viscosity of the fluids in these studies mentioned above covers only a small range, lower than the viscosity of viscous fluids occurred for many materials, biological, and petrochemical engineering.

Up to now, only a few data are available on bubble coalescence in microfluidic devices [25,26], and especially, the dynamics of bubble coalescence in highly viscous fluids with complex rheological properties in such devices has not been fully understood. The present work aims at studying experimentally the bubble coalescence in non-Newtonian fluids in a microfluidic expansion section. The measured flow fields around the aligned bubbles by a micro-PIV system, were employed to explore the mechanism of bubble coalescence.

2. Experimental procedures

The microfluidic device was fabricated in a plate ($46 \times 27 \times 2$ mm) of polymethyl methacrylate (PMMA) by precision milling and sealed with another thin PMMA plate. The configuration of the microfluidic device is depicted in Fig. 1. N_2 bubble was formed at the cross-junction by flow-focusing technique. After 14 mm of the cross-junction, there is an expansion section with an angle of $60°$. The axial length of the expansion is 20 mm. The cross section of the main channel and the two side channels is 400×400 μm. Gas was fed by a N_2 cylinder equipped with a pressure gage to stabilize the pressure. The gas flow rate was controlled by a high precision micrometering valve (Sagana Instrumentation, Luxembourg). Liquid was delivered from a 60 mL syringe by a syringe pump (Harvard Apparatus, USA).

A high speed digital camera CamRecord600 (up to 100,000 frames per second, Optronis GmbH, Germany) equipped with a microscopic magnification lens was set above the channel. In this work, 2000 fps and a shutter speed of 1/50000 s were used. The resolution of the pictures was 1280(H) × 256(V) pixels. A cold fiber light (Jeulin S.A., France), placed at the opposite side of the channel, was employed to illuminate the channel.

A micro-particle image velocimetry system (micro-PIV) (Dantec Dynamics, Denmark) was used by seeding the carrier fluid with 0.88 μm diameter calibrated Latex particles (Merck, France). The present work uses the 10× objective with a numerical aperture (NA) of 0.25. The flow was illuminated by a stroboscope. By shadowgraph of the seeding particles, images of the flow were taken by a double image digital camera through the microscope. The FlowMap software (Dantec Dynamics, Denmark) was employed to analyze the raw image pairs, resulting in reliable velocity fields.

N_2 was used as the gas phase. 0.5 wt% polyacrylamide (PAAm) (AN 913 SH, SNF Floerger, France) in demineralized water was used as non-Newtonian fluids. A Rheometrics Fluid Spectrometer RFS II (TA Instrument, USA) was employed to measure the rheological property. The 0.5 wt% PAAm solution behaved as shear-thinning fluids and could be fitted by the power-law model in the range of shear rates ($1–500$ s^{-1}) corresponding to the volumetric flow rates of the fluids: $\eta = K\dot{\gamma}^{n-1}$, where η is the viscosity of the fluids, K the consistency index (a measure of average viscosity), $\dot{\gamma}$ the shear rate, and n the flow index as a measure of deviation from the Newtonian fluid. For 0.5 wt% PAAm, $K = 2.87$ Pa s^n, $n = 0.35$.

3. Results and discussion

3.1. The two mechanisms for bubble coalescence

Two different mechanisms for bubble coalescence were observed at the expansion section (Fig. 2a and b). Mechanism I: the coalescence of two different bubbles. Mechanism II: one bubble firstly breaks into two different ones at the entrance of the expansion section, and then the two divided bubbles coalesce at the expansion area to form a new one. The types for bubble coalescence can be controlled by varying gas and liquid flow rates (Q_g and Q_l, respectively) (Fig. 3a). At a certain gas flow rate, the bubble coalescence switches from mechanism I to II, when the liquid flow rate increases to a threshold value. And the threshold liquid flow rate increases with the augmentation of the gas flow rate as shown in Fig. 3a. It is noteworthy that the Reynolds
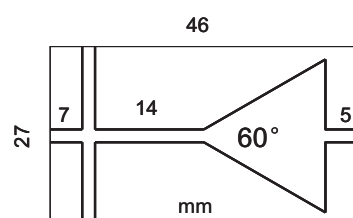

Fig. 1. The configuration of the microfluidic expansion device.